

## Data interpolation by angular weighted MWNI

Mark Ng\*, Divestco Inc., Calgary, Alberta, Canada

mark.ng@divestco.com

and

Dan Negut, Divestco Inc., Calgary, Alberta, Canada

### Summary

We propose to impose an extra angular weight function on the a priori model of the Minimum Weighted Norm Interpolation (MWNI). This can stabilize the inversion when it interpolates dipping reflectors under more severe unfavorable conditions such as meager data support or medium aliased conditions. The angular weights are derived from an angular search of the input amplitude spectrum in the frequency-wavenumber domain before the inversion begins.

### Introduction

Of many elegant and useful interpolation methods in seismic processing, recently MWNI has become a popular tool for seismic processing interpolation after it was introduced by Bin Liu and Sacchi (2004). It was then further extended into multi-spatial dimensions to be applied in real everyday processing situations by Daniel Trad (2009). Three major challenges of MWNI: (1) to recover large amount of missing data, (2) to upsample regularly missing data, and (3) to interpolate aliased dips. Since MWNI does a least-squares data fitting in space one frequency at a time, it uses the result from the immediate last frequency as a priori model for the present frequency. Usually MWNI starts from the stable low frequencies, and recursively works its way up to higher frequencies. This can get into unstable situations under aforementioned challenging scenarios because the previous frequency result may be an inadequate a priori model to use, and no knowledge from the high frequencies is utilized to help guide the inversion.

Naghizadeh (2012) suggested two ideas for data interpolation and de-noising: (1) a constraint which is an angular search in identifying dipping reflectors in order to make a mask for the dominant dips in the  $f-k_x$  domain and (2) perform a least-squares data fitting directly on the  $t-x$  data. This is not what MWNI would do. His method could be harsh on the data due to masking because masking requires parameterization skills to decide what to include or to reject.

Similar to his method, we will use the angular search by stacking the input data in the  $f-k_x$  domain; but in contrast, we will build an angular weighting function (not necessarily a mask). Furthermore, contrary to his method of imposing the angular mask in the  $f-k_x$  domain to fit the  $t-x$  data, we simply multiply the angular weights to the a priori model in  $k_x$  at the operating frequency  $f$  to fit the  $f-x$  data in the conventional MWNI method. The advantages of the proposed method are: less harshness to the resultant data, an easy 'plug-in' to any current conventional MWNI algorithm to improve performance, minimal added cost, and yielding good results.

### Method

Let  $d(x,t)$  be the observed input with missing data, and  $D(k_x,\omega)$  its corresponding 2D Fourier transform.

**Step 1.** Calculate an angular sum  $M(\theta)$  by summing the amplitude values in the radial direction starting from the origin of  $D(k_x=0, \omega=0)$  of all usable apparent dip angles  $\theta$ ;  $r$  is the radial length from the origin.

$$M(\theta) = \int_r |D(\theta, r)| dr \quad (1)$$

$$r = \sqrt{\omega^2 + k_x^2}, \theta = \tan^{-1} \frac{k_x}{\omega} \quad (2).$$

**Step 2:** Modify  $M(\theta)$ . One way is to change it into a mask value of 1.0 or a very small value depending on a threshold level  $q$  that can identify the major dips as Naghizadeh (2012) suggested giving  $M_q(\theta)$ . Or another alternative way proposed here, is to raise its power  $p$  in a range from 1 to 4 to give  $M^p(\theta)$ .  $p$  controls the level of emphasis in the presence of linear events, and a zero value places no emphasis.

**Step 3:** Get the angular weights gamma  $\gamma$  by populating  $M$  back to the  $f$ - $k_x$  domain even when the spectral component is aliased wrapping around and beyond the spatial Nyquist wavenumber. It is a very desirable key feature to protect the aliased dipping reflectors. Amplitude will be a constant in the radial direction, but may vary at different angles  $\theta$ .

$$\gamma(\omega, k_x) = M_q(\theta) \text{ or } M^p(\theta) \quad (3).$$

An example of gamma with a raised power  $p = 4$  is given in figure 1.

**Step 4:** Perform MWNI by imposing the angular weights  $\gamma$  to the very first a priori model amplitude spectrum  $\bar{D}$  at every frequency  $f$  for the data fitting in  $x$ . This provides a guide to the general impression of the dips. Then, apply the conjugate gradient (CG) method using the iteratively reweighted least-squares (IRLS) with a Cauchy norm to enhance sparsity in the transform model  $u_{k_x}$ . Note that the angular weights  $\gamma$  remain the same in the entire CG process. The adjoint operator at  $f$  is

$$u_{k_x} = [TF' \gamma \bar{D}]^H d_x = \gamma \bar{D} F T d_x \quad (4).$$

The forward operator for the approximate data is

$$\tilde{d}_x = [TF' \gamma \bar{D}] u_{k_x} \quad (5),$$

where  $u_{k_x}$  is the spatial transform model in  $k_x$ ,  $T$  the sampling diagonal only matrix,  $F'$  the inverse spatial Fourier transform operator,  $F$  the forward spatial Fourier transform operator,  $\bar{D}$  the slightly smoothed amplitude spatial spectrum of the input observed data  $d_x$ , and  $H$  the Hermitian transpose.

### Example 1: Recovering random missing data

The example shows how both the conventional MWNI method and the proposed angular weighted MWNI recover large amounts of missing data, 52% dead. Figure 2a is the input shot data in  $t$ - $x$  domain with missing data, and figure 2b, its corresponding noisy  $f$ - $x$  amplitude spectrum. Figure 3 shows a near perfect recovery result from a conventional MWNI. Figure 4 shows the recovery result by the proposed method using the threshold angular weighted MWNI. It is virtually identical to Figure 3. Usually, any MWNI performs well in random missing data situations.

### Example 2: Recovering large gap missing data

Figure 5a shows the input shot data with a large gap with 31% missing data in the center. Figure 6a shows that the conventional MWNI fails to recover the missing gap data, and figure 6b shows its corresponding unstable spectrum. Moreover, the amplitudes of the dipping reflectors everywhere are

weakened. Figure 7 shows the recovery result by the proposed method using the power angular weighted MWNI. Although not perfect, it is good and very usable in this challenging situation.

### Example 3: Recovering regularly decimated data, upsampling challenge

Figure 8a shows the input shot data in  $t$ - $x$  domain with regularly decimated data with 5 missing traces in between live traces, i.e. 84% missing data. Figure 8b shows its corresponding repetitive confusing highly aliased spectra. Figure 9a shows that the conventional MWNI fails to recover the decimated data at both dips giving a step-like response in both directions, and figure 9b shows its corresponding damaged spectrum. Figure 10 shows the recovery result by the proposed method using the power angular weighted MWNI. Although slightly noisy, the result is very usable in this demanding situation.

## Conclusions

Derived from the full frequency spectrum, the proposed simple angular weight function imposed on the a priori of MWNI can improve the ability to recover data under more adverse situations such a block gap of missing data, and upsampling, even for aliased conditions.

## References

- Liu, B, and M. D. Sacchi, 2004, Minimum weighted norm interpolation of seismic record: *Geophysics*, **69**, no. 6, 1560-1568.  
 Naghizadeh, M., 2012, Seismic data interpolation and denoising in the frequency-wavenumber domain: *Geophysics*, **77**, no. 2, V71-V81.  
 Trad, D, 2009, Five-dimension interpolation: Recovering from acquisition constraints: *Geophysics*, **74**, no. 6, V123-V132.

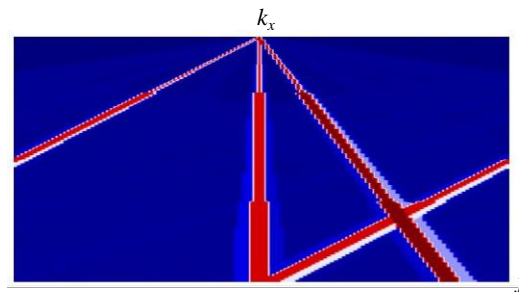


Figure 1: The 'power ( $p=4$ )' angular weights  $\gamma(\omega, k_x)$  amplitude spectrum derived from the confusing spectrum of figure 8 (b). The amplitude is constant in radial direction, but it can vary at different angles. The three red radial beams indicate that there are three linear reflectors. The red beam that wraps around the spatial Nyquist is necessary to track the aliased dipping reflector which has been crucially identified.

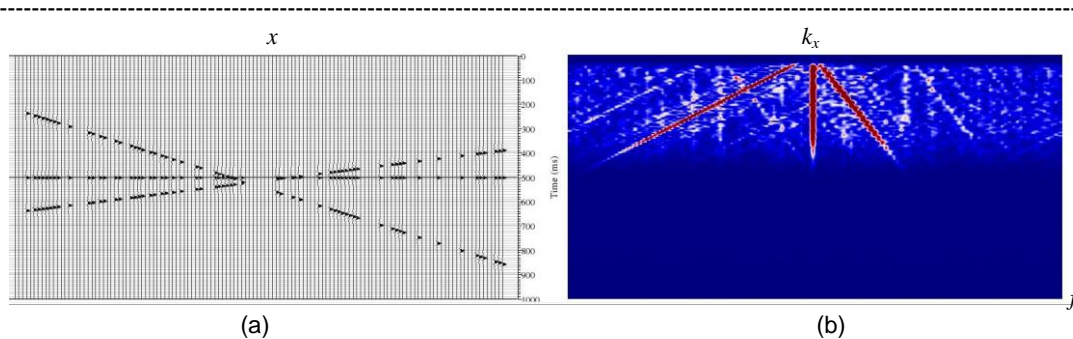


Figure 2: Example 1 - Input random 52% missing traces.  
 (a) The  $t$ - $x$  domain of a 128-trace shot data with three linear events with a slope of: 0 ms/trace, 2 ms/ trace and 5 ms/trace. The 5 ms/trace event is an aliased reflector even when there is no missing data. (b) Its corresponding  $f$ - $k_x$  domain amplitude spectrum reveals noisy random replicas of the ideal full data spectrum.

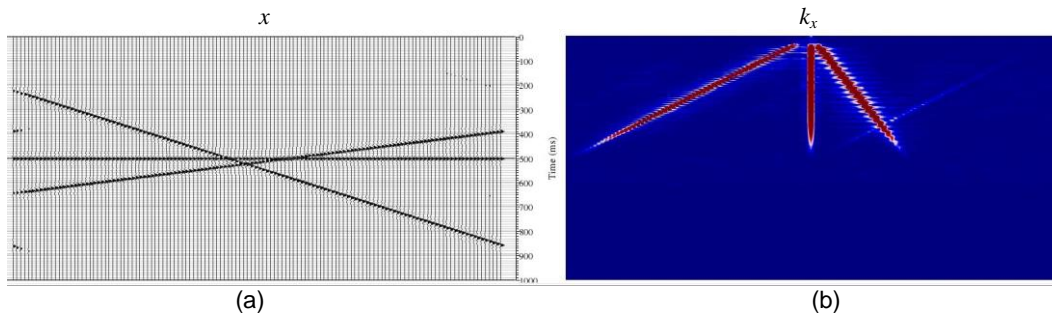


Figure 3: Example 1 – Conventional MWNI recovery of the random missing traces in figure 2. (a) The  $t-x$  domain of the recovered data with the missing traces nicely interpolated. It gives a near perfect result. (b) Its corresponding  $f-k_x$  domain amplitude spectrum reveals a single clean set of full spectrum.

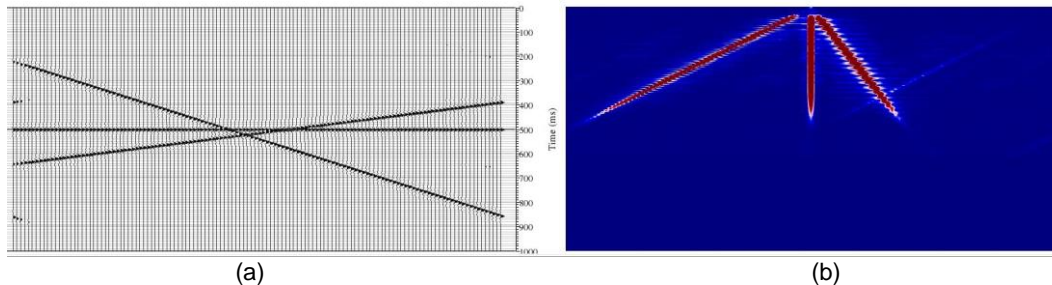


Figure 4: Example 1 – Proposed 'threshold' angular weights MWNI recovery of the random missing traces in figure 2. (a) The  $t-x$  domain of the recovered data with the missing traces nicely interpolated. It gives a near perfect result as does in figure 3 (a). (b) Its corresponding  $f-k_x$  domain amplitude spectrum reveals a single clean set of full spectrum.

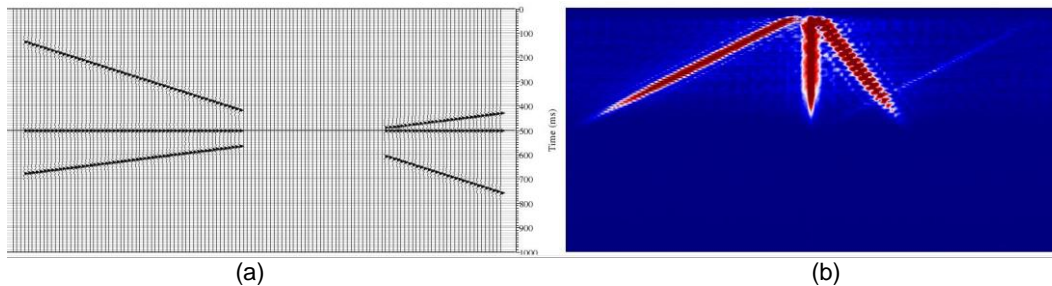


Figure 5: Example 2 - Input large gap with 31% missing data. (a) The  $t-x$  domain. (b) Its corresponding  $f-k_x$  domain amplitude spectrum reveals a widening of the wavenumber bands when compared to the full data spectrum (which is not shown here to save space, but it is virtually identical to figure 3 (b) or 4 (b)).

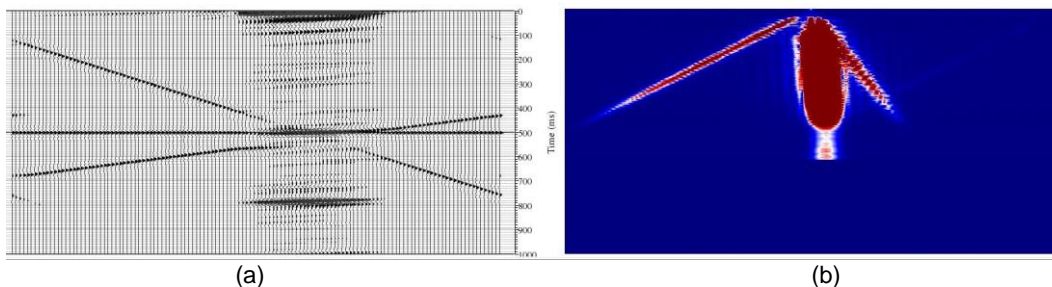


Figure 6: Example 2 – Conventional MWNI recovery of the large gap data in figure 5. (a) The  $t-x$  domain of the recovered data. It gives a completely erroneous interpolation result at the missing gap. The amplitudes of both dipping reflectors at the real data positions are about 20% weakened. (b) Its corresponding  $f-k_x$  domain amplitude spectrum confirms the unstable inversion result.

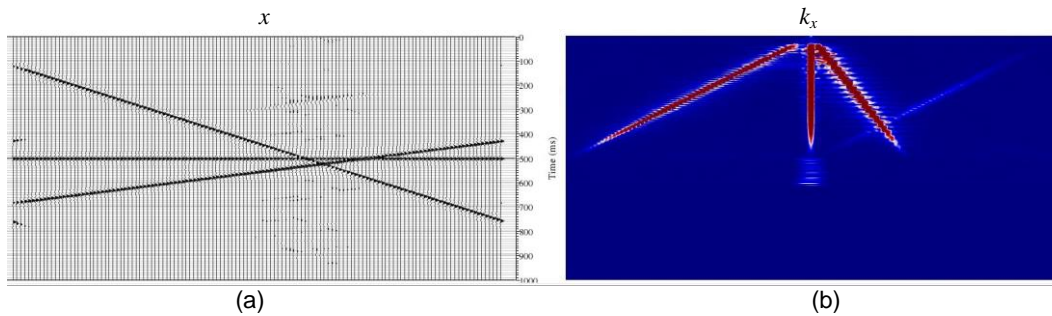


Figure 7: Example 2 – Proposed ‘power’ angular weighted MWNI recovery of the large gap data in figure 5. (a) The  $t$ - $x$  domain of the recovered data. It gives a reasonable interpolation result at the missing gap with some minor artifacts at the quiet zones. The amplitudes of both dipping reflectors are maintained. Although not perfect, the result is good and very usable in this challenging situation. (b) Its corresponding  $f$ - $k_x$  domain amplitude spectrum is good.

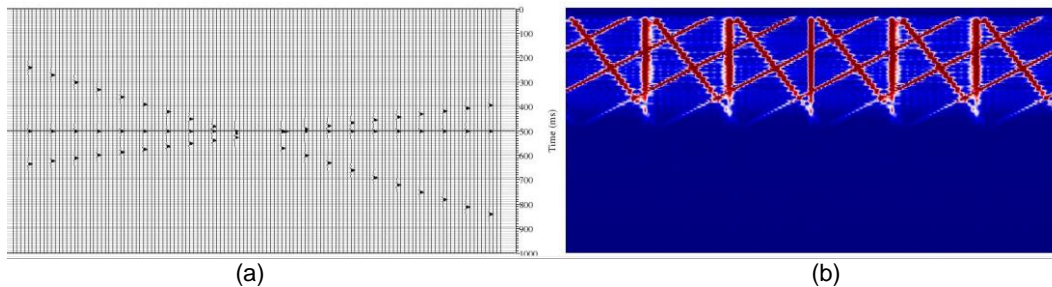


Figure 8: Example 3 - Input regularly decimated data: 5 missing traces in between live traces, i.e. 84% missing traces. (a) The  $t$ - $x$  domain. (b) Its corresponding  $f$ - $k_x$  domain amplitude spectrum reveals 5 replicas of the ideal full data spectrum; plus itself, a total of 6 aliased spectra.

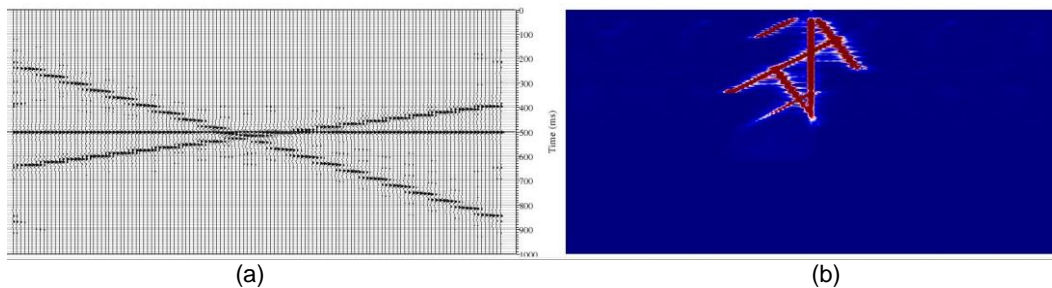


Figure 9: Example 3 – Conventional MWNI recovery of the regularly decimated data in figure 8. (a) The  $t$ - $x$  domain of the recovered data. It shows that the interpolation of the decimated data fails giving a step-like response in both dips. (b) Its corresponding  $f$ - $k_x$  domain amplitude spectrum reveals the broken spectral components containing spectral leakage from aliased replicas.

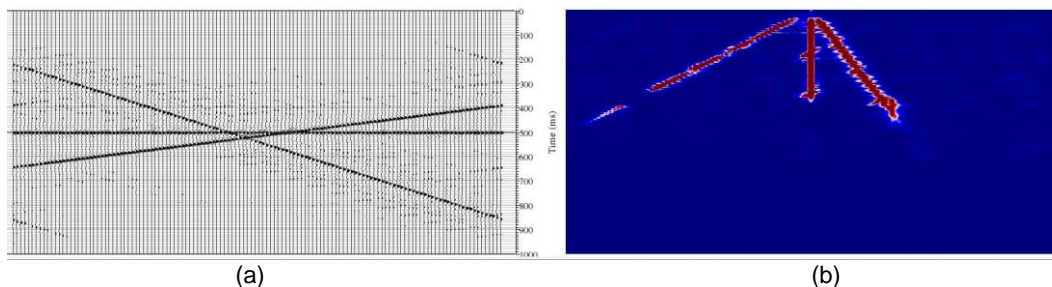


Figure 10: Example 3 – Proposed ‘power’ angular weighted MWNI recovery of the regularly decimated data in figure 8. (a) The  $t$ - $x$  domain of the recovered data. Although slightly noisy, the result is very usable in this demanding situation. (b) Its corresponding  $f$ - $k_x$  domain amplitude spectrum reveals a reasonable recovery of full data spectral form with some chattering. The power angular weights  $\gamma$  designed from figure 8 (b) is shown in figure 1.